Integrated protein-protein interaction and RNA interference screens reveal novel restriction and dependency factors for a tick-borne flavivirus in its human host

Marion Sourisseau[1], Yves Unterfinger[1], Manon Lemasson[1#], Maxime Chazal[2], Ségolène Gracias[2], Gregory Caignard[1], François Piumi[1], Axel Grot[1], Sara Moutailler[3], Damien Vitour[1], Nolwenn Jouvenet[2], Muriel Coulpier[1], Sandrine A. Lacour[1], Jennifer Richardson[1*]

[1]UMR Virologie ANSES, ENVA, INRAE, Maisons-Alfort, France.

[2]Virus Sensing and Signaling Unit, CNRS UMR3569, Institut Pasteur, Université de Paris Cité, Paris, France

[3]UMR BIPAR ANSES, ENVA, INRAE, Maisons-Alfort, France.

[#]Current address: Phagos, 5 avenue du Général de Gaulle, 94160 Saint-Mandé, France

*Correspondance : jennifer.richardson@vet-alfort.fr

ABSTRACT

In Europe, tick-borne encephalitis virus (TBEV) is responsible for severe neurological disease in humans. Like other viruses, TBEV is an obligate intracellular life form whose survival requires subversion of metabolic processes and evasion of anti-viral pathways. This feat is achieved in no small part by binary interactions between dedicated viral proteins and host proteins. Such protein-protein interactions (PPI) constitute molecular determinants of critical pathobiologic traits of viruses, including host-range, zoonotic potential and virulence, and represent realistic targets for anti-viral therapies.

To shed light on the pathobiology of TBEV in human, we have resolved the network of PPI established with its human host by interaction proteomics. A high-throughput screen for virus-host PPI was performed involving the complete set of open reading frames of TBEV and the cDNA libraries of *Homo sapiens*, by means of yeast two-hybrid methodology. We have discovered a large set of virus-host protein-protein interactions concerning 42 different human proteins directly interacting with nine viral proteins. Many of these human interactors have never been linked in the literature to viral infection.

The functional significance of the host interactors in viral infection as viral dependency or restriction factors was then characterized *in vitro* by RNA interference, and their function inferred by bioinformatic analysis. Approximately 40% of the identified human proteins have a significative impact on TBEV viral replication. These are engaged in many biological processes, whose involvement in viral infection is expected for many, but enigmatic for some. Further work will be necessary to gain molecular understanding of how these biological processes support or restrict TBEV replication, and whether they constitute viral vulnerabilities that can be exploited therapeutically.

INTRODUCTION

Flaviviruses, which are principally transmitted by mosquitoes and ticks, cause devastating human diseases such as Dengue fever in the tropics and subtropics and are a constant source of emerging pathogens of pandemic potential, for which ZIKA and Usutu viruses may serve as recent examples. In Europe, a tick-borne flavivirus – the Tick-borne encephalitis virus (TBEV) – is the most significant arbovirus from a medical perspective. Some 3000 cases of TBEV infection, frequently associated with severe central nervous system disease in humans, are reported in Europe each year. Moreover, TBEV is an emerging pathogen on the European continent, as the endemic zone has expanded and the reported incidence increased in many endemic countries[1]. Transmission of TBEV is principally transmitted by the major European tick *Ixodes ricinus*, but may also be food-borne, as TBEV may be acquired by consumption of raw milk and its derivatives from infected sheep and goats in areas where TBE is endemic. Though effective vaccines exist for TBE, they are insufficiently deployed, and antiviral therapy is currently unavailable.

Like all viruses, flaviviruses are obligate intracellular life forms whose survival requires subversion of metabolic circuits and evasion of anti-viral pathways. Within the cell, these pathways are embedded in extensive protein-protein interaction (PPI) networks[2], and their misappropriation by viruses is largely mediated by binary interactions between dedicated viral proteins and critical network proteins. Indeed, the host proteins targeted by viral proteins tend to occupy positions in the PINs with particular topological features, such that the functional impact of a single interaction may be felt well beyond its immediate neighbourhood by transmission along the cascade of interactions within the PIN[3]. Virus-host PPI thus represent molecular determinants of critical pathobiologic traits of flaviviruses, including host-range, zoonotic potential and virulence. Such interactions represent realistic targets for anti-viral therapies, thus providing a compelling reason to resolve the complete set of virus-cell interactions at the molecular level.

For mosquito-borne flaviviruses of medical significance, virus-host interactions and PPIs in particular have come under intensive study, principally by means of yeast two-hybrid methodology (Y2H) or affinity purification coupled with mass spectrometry (AP-MS)[4,5]. Translation of the flaviviral RNA genome yields a single polyprotein precursor that is cleaved by viral and cellular proteases into three structural (Capsid, prM and Env) and seven non-structural (NS1, NS2A, NS2B, NS3, NS4A, NS4B and NS5) proteins. These have been used in several high-throughput studies to explore PPIs in Y2H[6,7] or AP-MS[8,9] screens. The PPIs established between viral and cellular proteins represent molecular effectors of an evolutionary stalemate, certain interactions being conducive while others deleterious to viral survival, and thus representing host “dependency” or “restriction” factors, respectively. Moreover, mapping of

PPIs has served to reveal putative molecular determinants of distinct pathobiologic features, such as induction of microcephaly by Zika virus (ZIKV)[8], as well as druggable targets[9].

Thus far, the molecular mechanisms that underlie pathobiologic traits have been far less studied in tick-borne flaviviruses than in their mosquito-borne counterparts. A single published study describes a Y2H screen involving the NS3 and NS5 proteins of TBEV and human cDNA libraries[7]. The putative interactions were functionally annotated using *in silico* tools, but their validity was not examined at the biochemical level and their functional implication, such as for viral replication, was not addressed.

In the present study we have performed a high throughput Y2H screen for PPI involving the entire set of open reading frames for the most medically significant arbovirus in Europe, TBEV, and a cDNA library derived from its human host. A set of TBEV-human host PPIs were discovered, many of which having never been previously described for other virus-host systems. The functional significance of the human interactors in viral infection was systematically investigated by performing an RNA interference screen. Many of these interactors were discovered to represent viral restriction or dependency factors – most of which having never been assigned a functional role in other viral infections. The significance of these interactions for the pathobiology of TBEV, in relation to the presumed functional role of the human interactors, is discussed. Our study thus illuminates the strategies by which tick-borne flaviviruses control cellular processes and cause disease, and should ultimately contribute to disclosing viral vulnerabilities that can be exploited therapeutically.

RESULTS

The TBEV – *Homo sapiens* protein-protein interaction network

In order to resolve the PPI network between TBEV and its human host, a *H. sapiens* cDNA library was screened by Y2H assay for binary PPI with the complete set of ORFs of TBEV. These encoded the three major structural – C, prM, and E – and eight nonstructural proteins – NS1, NS2A, NS2B, NS3, NS4A, 2K, NS4B and NS5 (Fig. 1a). ORFs encoding the cleavage products of full-length prM, namely, the mature M protein and the cleaved N-terminal portion (prM') of prM, were used separately for screening. Among 231 yeast colonies selected for sequencing, 27 human proteins interacting with TBEV bait proteins were identified. Of note, the screen described in the current report was performed concomitantly with a Y2H screen for PPI between the *H. sapiens* proteome and the complete set of ORFs of the Louping Ill virus (LIV), a tick-borne flavivirus closely related to TBEV and an important pathogen in sheep, as well as with Y2H screens for PPI between the *Bos taurus* proteome and the complete set of ORFs of both TBEV and LIV (data not shown). Based on PPI disclosed between LIV bait proteins and human prey or between TBEV bait proteins and bovine preys in these independent Y2H screens, orthologous PPI between TBEV bait proteins and certain human proteins were specifically evaluated by Gap repair (GR) assay (Fig. 1b).

PPI observed in the original TBEV - H. sapiens screen supported by retrieval of a single sequence were also evaluated by GR. This strategy let to confirmation of nine human proteins originally identified in the TBEV-human host Y2H screen as interacting with TBEV bait proteins, and to identification of fifteen additional human proteins that interact with TBEV bait proteins (Supplementary Table 1). The resulting set of 42 human prey proteins are shown in a network representation in which nodes, representing proteins, are connected by edges, representing binary PPI (Fig. 2a). Nine nodes represent viral bait proteins, while 42 represent human preys. Among these last, 20 interacted with NS5, 13 with prM', 3 with NS2B, 2 with C and one each with M, NS1, NS3 and NS4A and 2K (Fig. 2b). One human prey protein, encoded by the UBQLN1 gene, interacted with both 2K and NS2B proteins. PPI were not evidenced for E, NS2A and NS4B proteins.

Overlap of PPI with published TBEV-*H. sapiens* PPI

In a previous study, a Y2H screen had been carried out between the NS3 and NS5 proteins of TBEV (strain 263[10]) and human cDNA libraries[7]. Full-length NS5, as well as domains thereof responsible for RNA polymerase and methyltransferase functions, were used separately for screening. The set of human proteins interacting with NS5 (NS5 bait set) from Le Breton *et al.*[7] and the present study were merged (Fig. 3a). Of the 33 and 20 human prey revealed in the former and present study for NS5, respectively, only 3 – encoded by GOPC, SCRIB and TYK2 genes – were common to both studies.

Biological processes engaged by TBEV infection

To identify the biological processes engaged by TBEV infection, g:Profiler[11] was used to retrieve enriched Gene ontology terms for the human prey proteins disclosed in the present study. Enrichment analyses of the prey proteins, collectively or by individual bait set, retrieved few or no enriched GO terms, respectively, that attained statistical significance. Thus, to identify major biological processes engaged by TBEV infection, the same analyses were performed for individual bait sets after extension of each set by the addition of up to ten human proteins (Supplementary Table 2) that physically interact with each prey in the bait set (Fig. 4b), as retrieved from STRING[12].

Multiple enriched GO terms that attained statistical significance were retrieved for the STRING-extended bait sets (Supplementary Table 3). Those concerning the most salient biological processes are shown for individual bait sets in Fig. 4a and illustrated in network format in Fig. 4b. Among them, we identified certain cellular processes with evident links to viral infection, such as cytoskeleton component-based processes (NS5, prM' and M), vesicle transport (C and prM'), translation (NS2B, NS5), apoptotic processes (NS3), protein degradation (NS2B) and innate immune response (NS5) (Fig. 4 and Supplementary Table 3). Of note, enriched GO terms displayed little overlap between extended bait sets, suggesting that the biological processes engaged by individual viral proteins are largely distinct.

Functional analysis of TBEV-human host PPI

To assess the role of the human prey proteins identified in the present study in the TBEV life cycle, we analyzed the consequence for viral replication of silencing their expression by RNA interference (RNAi). Small interfering RNA (siRNA) was used to transfect A549 cells prior to infection with TBEV. Viral replication was assessed 24h after infection by quantification of infectious particles released into the supernatant (Fig. 5a). Transfection with irrelevant (non-targeting) siRNA (siNT) was used to provide a reference value. Infectious titers measured after silencing with siRNA specific for individual human prey proteins were expressed relative to titers measured after treatment with siNT, and plotted against their respective p-value. When a specific siRNA induced at least a two-fold change in normalized infectivity with a p-value <0.01, the targeted host factor was considered a hit. Host factors whose silencing diminished titers were considered to represent dependency factors, while those whose silencing augmented titers were considered to represent restriction factors.

As expected, siRNA directed against the restriction and dependency control proteins IFNAR2 and VIM[13] modulated infection accordingly. Small interfering RNA against IFNAR2 induced a 13-fold increase in viral release, while VIM extinction significantly decreased infectivity titers by a 5.3-fold factor. Among the 42 host proteins tested (Supplementary Table 4), the silencing of 19 of them significantly modulated infectious particle release by 2-fold or greater, as compared with the reference titer (Fig. 5b).

Eleven hits for which silencing negatively affected TBEV release (encoded by SPAG5, FHL2, BRI3BP, TCEB2, TRIOBP, DYNLL1, DYNLL2, UBQLN1, RPL37A, RPL13A and SCRIB genes) may be considered to represent TBEV dependency factors. Six factors, for which silencing enhanced TBEV release by more than 2-fold, qualified as restriction factors (encoded by PUM2, SPDL1, APIP, KIF15, ALX1 and SBNO1 genes).

DISCUSSION

In comparison with their mosquito-borne counterparts, tick-borne flaviviruses are notoriously understudied, including as regards the PPI established between viral and host proteins, which permit viruses to co-opt biological circuits and circumvent the host's antiviral response. In the present study we have performed a Y2H screen between the most medically important arbovirus in Europe, TBEV, and its human host, thereby revealing multiple hitherto unknown PPI. The functional role of the human interactors ("prey proteins") was systematically addressed by RNA interference, disclosing multiple viral restriction and dependency factors, many of which undescribed for other viruses.

Among the 42 human prey proteins of TBEV revealed in the present Y2H screen and associated gap repair analyses, 6 (14%) and 11 (26%) were found to be restriction and dependency factors, respectively. Thus, a high proportion (≈ 40%) of human proteins that physically interact with TBEV proteins could be

shown to have a measurable impact on viral replication. This percentage is likely to be underestimated, as knockdown of certain proteins may have been inadequate, due for example to high levels of mRNA or to an extended half-life of the protein product. Moreover, knockdown of certain proteins may have been compensated by non-targeted human proteins playing a redundant role in viral replication.

Of the three structural proteins of TBEV that were used for screening, C, prM (as its cleaved products prM' and M) and E, human prey proteins were discovered for C, prM' and M. Following expression of the precursor polyprotein of flaviviruses in the ER membrane and cleavage by the viral protease, the C protein persists as an ER membrane-anchored protein facing into the cytosol, until further proteolytic cleavage releases soluble C into the cytosol. The mature form of flaviviral C may strongly associate with the ER-derived membranes at the site of viral replication[14], but can also be imported into the nucleus[15]. Both of the human prey proteins found for TBEV C protein – Angiotensin II Receptor Associated Protein or AGTRAP and BRI3 (Brain protein I3) Binding Protein (BRI3BP) – are multi-pass membrane proteins. The latter was found to be a dependency factor. To the best of our knowledge, neither protein has previously been found to bind to viral proteins or to play a role in viral replication. BRI3BP, presumed to be principally expressed in the mitochondrial membrane, is virtually uncharacterized, though one study suggests that it might have pro-apoptotic activity[16].

Immature flaviviral particles bud into the lumen of the ER and follow the exocytosis pathway for ultimate egress via the plasma membrane. During viral trafficking the prM protein of flaviviruses is expressed as a membrane-anchored protein, until cleavage by the cellular endoprotease furin in the trans-golgi network releases the NH2-terminal portion, prM', into the ER lumen, leaving the mature M protein anchored in the viral membrane. Twelve prey proteins were evidenced for the prM' moiety; namely, Apoptotic peptidase activating factor 1 interacting protein (APIP), Diacylglycerol kinase delta (DGKD), DnaJ heat shock protein family (Hsp40) Member B4 (DNAJB4), dynein light chain 1, cytoplasmic (DYNLL1), Dynein light chain 2, cytoplasmic (DYNLL2), Dynein light chain Tctex-type 1 (DYNLT1), Filamin C (FLNC), Histone methyl-lysine binding protein 3 (L3MBTL), RAB Interacting Factor (RABIF), c-Rel (REL), SERTA domain-containing protein 1 (SERTAD1), Suppressor of variegation 4-20 homolog 1 (SUV420H1) and X antigen family member 1 (XAGE1B). Among these twelve human prey proteins, APIP was revealed to be a viral restriction factor, while the paralogs DYNLL1 and DYNLL2 were evidenced as dependency factors. To the best of our knowledge, APIP has not previously been reported to bind to viral proteins or to play a role in viral replication. APIP is a 5-methylthioribulose-1-phosphate dehydratase belonging to the methionine salvage pathway[17,18], and an inhibitor of both apoptosis and pyroptosis[17].

The dynein light chains DYNLL1, DYNLL2 and DYNLT1 are non-catalytic accessory components of the cytoplasmic dynein 1 complex, and presumed to link dynein to various cargos for retrograde motility of vesicles along microtubules. Various proteins have been shown to physically interact with dynein light

chains (for review see [19]). Our previous study disclosed a physical interaction between the prM' moiety of TBEV and the DYNLL1 ortholog in the tick *Ixodes ricinus*[20], suggesting that the interaction, and possibly functional role, is conserved across in the arboviral life cycle between mammalian host and arthropod vector.

A member of the NF-κB family of transcription factors, the c-Rel protein is involved in the innate immune response to myriad viruses, and has been shown to physically interact with the Tax protein of human T-cell leukemia virus[21]. The transcriptional factor SERTAD1 has been shown to interact with the E2 protein of Classical swine fever virus[22], a member of the genus *Pestivirus* in the family *Flaviviridae*, and ablation of the interaction restricts replication in cellular models and *in vivo* in swine[23]. SUV420H1, a dimethyl transferase of histone H4, has been described to be involved in the latency of Epstein barr virus[24]. The remaining human prey proteins of prM', DGKD, DNAJB4, FLNC, L3MBTL3 and RABIF, have not, to our best knowledge, been implicated as intervening in the life cycle of viruses.

Of the 8 ORFs encoding nonstructural proteins of TBEV that were used for screening, human prey proteins were discovered for NS1, NS2B, NS3, NS4A, 2K and NS5.

ALX homeobox protein 1 (ALX1), the unique interactor of NS1 in our Y2H screen, exerts a negative impact on TBEV infection. This transcription factor has been shown to play a critical role in coordinating the antiviral innate immune response, along with known virus activated factors such as IRF3, IRF7, STAT1, and/or NF-kB[25].

Three human prey proteins were discovered for the NS2B protein; namely, the ribosomal protein S7 (RPS7) and two members of the ubiquilin family (UBQLN1 and UBQLN4), UBQLN1 being identified as a dependency factor for TBEV. Ubiquilins behave as adaptor proteins that target poly-ubiquinated proteins to the proteosome for degradation, and have also been implicated in autophagy and endoplasmic reticulum-associated protein degradation (reviewed in [26]). Of note, proteins of several viruses have been found to interact with ubiquilin family members[27,28,29], in some cases providing benefit for viral replication[29]. In our previous study, the tick *I. ricinus* ortholog of ubiquilin-1 (UBQLN1 gene), was found by Y2H to be an interactor of TBEV NS4A[20], suggesting that co-opting of ubiquilin by TBEV may be conserved in its mammalian host and arthropod vector.

The NS3 protein is not only a viral protease required for cleavage of the viral polyprotein precursor and of release of individual nonstructural proteins, but also an RNA helicase involved in viral RNA synthesis[30,31]. Four-and-a-half LIM domain protein 2 (FHL2), the sole interactor of NS3 in our Y2H screen, was identified as a dependency factor for TBEV. FHL2 has been shown to be implicated in apoptosis[32,33], a process shown to be modulated by NS3 protein of multiple flaviviruses[34,35].

The TBEV NS5 protein plays an essential role in viral replication as both a methyltransferase and an RNA-dependent RNA polymerase. By inhibiting the type-I IFN pathway, it also plays on important role in immune evasion[36–38]. Twenty human prey proteins were evidenced for the TBEV protein (see Fig 3); of which 6 and 3 were identified as dependency and restriction factors, respectively. Dependency factors included the ribosomal proteins L37A and L13A (RPL37A and RPL13A, respectively), Scribble (SCRIB), TRIO And F-Actin Binding Protein (TRIOBP), Elongin B (TCEB2) and Sperm Associated Antigen 5 (SPAG5), while Strawberry Notch 1 (SBNO1), Kinesin Family Member 15 (KIF15) and Spindle Apparatus Coiled-Coil Protein 1 (SPDL1) behaved as restriction factors.

Regarding the dependency factors that bound to NS5, both RPL37A and RPL13A are components of the large 60S subunit, with the latter playing a role in downregulation of the inflammatory gene expression as a component of the IFN-gamma-activated inhibitor of translation (GAIT) complex (reviewed in [39]). RPL13A silencing also impacts replication of influenza[40]. The physical association between NS5 and SCRIB, previously described in Le Breton *et al.*[7], has been suggested to antagonize the innate immune response by impeding interferon-stimulated JAK-STAT signalling[41]. The present study, however, is the first to evidence an impact for SCRIB in TBEV infection.

TRIOBP interacts with the protein Trio, implicated in neural tissue development, organization of the actin cytoskeleton, cell motility and cell growth and with F-actin, with no described role in viral infection up to now. TCEB2 is a regulatory subunit of the transcription factor B (SIII) complex, known to be subverted by HIV to co-opt proteosomal degradation pathways to counteract cellular restriction factors[42]

SPAG5, originally identified as a microtubule-associated protein with dual localization to both centrosomes and kinetochores, is required for centrosome integrity, mitotic spindle formation and chromosome segregation during mitosis[43,44]. It also has an independent role in regulating apoptosis induced by cell stress[43,44]. NS5 of Dengue and ZIKA viruses (DENV and ZIKV) are known to localize at centrosomes during cell division[45,46]. While formation of the ZIKV viroplasm is closely associated with the centrosome and the Golgi MTOC[47], neither viroplasm formation nor virus production are significantly impaired in the absence of centrosomes. Thus, the functional significance of interactions between flavivirus proteins with centrosomes remains ill-defined.

Regarding the dependency factors that bound to NS5, SBNO1 has been shown to associate with nonstructural viral proteins from several RNA+ viruses, such as ZIKV NS4A and NS5[8,48], as well as Sars-Cov2 Nsp12[49]. Orthologs of SBNO1 are implicated in nervous system development involving the Notch pathway, or in activation of Notch signaling pathways in zebrafish[50,51] and *Drosophila*[53–55], respectively. ZIKV interferes with neuronal differentiation by dysregulating the canonical Notch signalling pathway, both in cultures of hNPCs and in mouse embryonic brains[52]. An impact for SBNO1 on viral replication,

however, had never previously been reported. The two remaining NS5-binding restriction factors, KIF15 and SPDL1, both located in kinetochores, have not previously been linked to viral infection.

In conclusion, our study has disclosed novel PPIs for a highly significant European arbovirus and revealed multiple viral restriction and dependency factors, some shared with other viruses while others never previously described in the published literature. Beyond elucidation of the strategies by which tick-borne flaviviruses control cellular processes and cause disease, our study sheds light on the cellular function of certain host interactors whose biological role is as yet enigmatic.

ACKNOWLEDGEMENTS

This study was made possible by a grant from the French national research agency (Project N° ANR-19-CE35-0015-01). The Ph.D. of ML was financed by a grant from the French Agency for Food, Environmental and Occupational Health & Safety (ANSES, Grant No. PHD2017-2020). MS received post-doctoral funding from the DIM1Health. The Ph.D. of AG is financed by the LabEx *Integrative Biology of Emerging Infectious Diseases*.

AUTHORS' CONTRIBUTIONS

JR, SAL, MuC, NJ and MS conceived and designed the study. MS, YU, MaC, SG, ML and AG carried out the wet lab experiments and/or bioinformatic analyses. GC and DV provided guidance and assistance with the Y2H screen. FP provided support for bioinformatic analyses. SM provided an essential resource. The paper was drafted by JR and MS and revised by DV, GC, ML, MuC and SM. All authors read and approved the final manuscript.

MATERIALS & METHODS

Cell culture

The simian epithelial cell line Vero (ATCC No. CCL-81), used for propagation and titration of TBEV, and the human epithelial cell line A549 (ATCC No. CCL-185) were cultivated in Dulbecco's modified Eagle's medium (DMEM; Gibco BRL Life Technologies, Gaithersburg, MD) supplemented with 5% fetal calf serum (FCS) (Eurobio) and 100 U/ml penicillin and 100 µg/ml streptomycin (both from Gibco BRL Life Technologies). Cells were maintained at 37°C in the presence of 5% CO_2.

Viral propagation and quantification

The Hypr strain of TBEV (GenBank accession number U39292.1), isolated in the Czech Republic from a child with TBE[53], was propagated and titrated in Vero cells grown in DMEM supplemented with antibiotics as described above and 2% FCS. Viral stocks were prepared as described in Lemasson *et al*.[20] and quantified by endpoint dilution assay on Vero cells, as visualized by the virus-induced cytopathic effect (CPE), as previously described[54]. Briefly, 1.5×10^4 Vero cells were seeded in 100 µL of DMEM supplemented with antibiotics and 2% FCS in wells of a 96-well plate the day prior to infection with 25 µL of serial dilutions of virus in medium as above (6 wells per dilution). Five days post-infection, infected wells were scored for evidence of virus-induced CPE. The fifty percent tissue culture dose ($TCID_{50}$) was calculated according to the method of Reed and Muench[55].

Yeast two-hybrid screen

In order to identify human proteins that physically interact with TBEV proteins, a yeast two-hybrid (Y2H) screen[56] was performed. To this end, the coding sequences of all open reading frames of TBEV Hypr were cloned and recombined into the pPC97 plasmid (Invitrogen) downstream of the DNA-binding domain of the Gal4 transcription factor (Gal4-DB; Fig. 1), as described in Lemasson *et al*.[20]. Of note, ORFs encoding the cleavage products of full-length prM, namely, the mature M protein and the cleaved N-terminal portion (prM') of prM, rather than the entire prM protein, were used separately for screening. A human cDNA library, in which cDNA derived from A549 cells had been cloned within the pDEST22 plasmid (Invitrogen) for in frame expression downstream of the activation domain of Gal4 (Gal4-AD), was kindly provided by Pierre-Olivier Vidalain. After transformation of the Y2H Gold and Y187 yeast strains with pPC97 constructs encoding viral baits and the cDNA library encoding *H. sapiens* preys, respectively, the Y2H screen was conducted essentially as described by Lemasson *et al*[20]. The TBEV-*H. sapiens* screen was part of a broader screen in which viral bait proteins from not only TBEV but also from the highly related Louping Ill virus (LIV) were used to screen cDNA libraries from not only *H. sapiens*, but also *Bos taurus* species. The cloning of LIV baits and the derivation of the *B. taurus* cDNA library have been described in Lemasson *et al*.[20] and Fablet *et al*.[57] , respectively.

Gap Repair

To determine whether PPI identified for proteins of LIV but not TBEV in Y2H screens of the human cDNA library were actually shared by the two viruses, interaction between the orthologous TBEV proteins and LIV-binding prey was evaluated by gap repair (GR) assay[58] as described in Lemasson *et al*[20]. Briefly, yeast carrying plasmids expressing DB-fused viral proteins were co-transformed with 10 ng of linearized pPC86 plasmid and 3 µL of PCR product encoding the protein of interest (as produced during the Y2H screen) and plated on medium lacking leucine (leu) and tryptophan (trp) and then transferred to

medium differing by the absence of histidine (his) and the presence of 5 mM 3-amino-1,2,4-triazole (3-AT; Sigma-Aldrich, Saint- Louis, MO, USA). Homologous recombination between pPC86 and the PCR product then reconstituted the expression cassette encoding the AD-fused prey protein, and growth on medium lacking leu, trp and his was conditioned by physical interaction between viral and *H. sapiens* proteins. A similar strategy was used to determine whether PPI identified in Y2H screens for LIV or TBEV with the bovine but not human cDNA library were actually shared by the two mammalian species. In brief, based on sequence analysis of the PCR products corresponding to bovine prey, the orthologous regions of human cDNA were amplified from mRNA of A549 cells by RT-PCR. These PCR products were then used in GR assay as described above.

RNAi Screen

RNAi targeting the 42 human proteins (a pool of 4 siRNA for each target) recovered in the Y2H assay (RNAi sequences provided in Supplementary Table 4) was purchased from Horizon Discovery (Cherry-pick Library in SMARTpool format). Three days prior to transfection, 10^4 A549 cells were seeded in wells of 48-well plates. Transfection was performed in triplicate with 25 nM of siRNA and 1 µL of DharmaFECT 1 Transfection reagent (Horizon Discovery) as per manufacturer's instructions. Forty-eight hours post-transfection, RNAi-transfected cells were infected with TBEV Hypr at an MOI of 0.5 $TCID_{50}$ per cell in DMEM supplemented with antibiotics 2% FCS. Viral inoculum was removed 90 minutes later, and cells were washed twice with PBS before addition of 200 µL of medium as above. Supernatants were collected 24h post-infection. The impact of RNAi on viral infection was assessed by quantification of infectious particles in supernatants of A549 cells by endpoint dilution assay on Vero cells, and expressed in $TCID_{50}$ as the mean of biological triplicates.

Cell viability after knockdown was evaluated for each siRNA pool in the absence of infection, 48h post-transfection of A549, by using commercially available reagents (Cell Titer Glo Luminescent Cell Viability Assay; Promega) according to the manufacturer's instructions (data not shown).

In silico and Gene Ontology (GO) analyses

PPI were graphically represented using Cytoscape software[59]. The g:GOSt tool of g:Profiler [11](https://biit.cs.ut.ee/gprofiler/gost) was used for functional enrichment analysis of our bait-sets, using g:SCS algorithm with a defined p-value threshold of 0.01. Human prey proteins were submitted to the Gene Ontology (GO) term enrichment service using an *H. sapiens* organism filter to identify biological processes enriched in the yeast two-hybrid dataset. As few statistically significant terms were recovered, sets of human prey proteins for individual viral bait proteins ("bait sets") were extended by retrieval of up to 10 physical PPI for each prey of each bait set from the STRING database[12], using the

Cytoscape StringApp[60]. The list of GO terms and associated p-values was condensed by using the REVIGO (reduce and visualize Gene Ontology; http://revigo.irb. hr/)[61].

Statistical analyses

Data from the siRNA screen were analyzed for statistical significance with Prism9 software (GraphPad Software) using the Mann-Whitney test. A p-value < 0.01 was considered significant. Values represent the mean and standard deviation (SD) of at least two independent experiments, each performed in biological triplicate.

Enriched GO terms were obtained using the g:SCS (Set Counts and Sizes) correction method. Adjusted p-values < 0.01 were considered significant.

FIGURE LEGENDS

Fig.1 **Yeast two-hybrid (Y2H) workflow for discovery of TBEV-human host protein-protein interactions. a,** Schematic representation of the TBEV RNA genome depicting viral ORFs cloned downstream of the DNA-binding domain (DB) of the Gal4 transcription factor, for expression of viral baits in the Y2H screen. **b,** Experimental workflow for Y2H screens and gap repair assays.

Fig.2 **TBEV-human host protein-protein interactions revealed by Y2H. a,** TBEV-human host protein-protein interaction (PPI) network. Nodes and edges represent proteins (viral bait and human prey) and PPI, respectively. Regarding edges, dots, equal dashes and solid line types represent PPI identified by gap repair (GR) only, by Y2H only or by both GR and Y2H, respectively. Sine waves represent physical PPI between human prey proteins retrieved from the STRING database[12]. **b,** Number of distinct *H. sapiens* prey proteins identified for each viral bait protein.

Fig.3 **Comparison of TBEV NS5-human host protein-protein interactions uncovered in independent Y2H screens. a,** TBEV NS5-human host PPI network including data from both Le Breton *et al.*[7] and the present study. Nodes and edges represent proteins (TBEV NS5 and human prey) and PPI, respectively. Nodes with purple or white fill colour represent prey proteins found only by Le Breton *at al.*[7] or only in the present study, respectively, while nodes with yellow fill colour represent prey proteins found in both studies. Sine waves represent physical PPI between human prey proteins retrieved from STRING[12]. **b,** Venn diagram showing overlap (yellow) in human prey proteins identified in Le Breton *et al.*[7] (purple) and in the present study (white).

Fig.4 **Functional annotation of extended TBEV-human host protein-protein interaction network.** Extended TBEV-human host PPI network displaying Gene Ontology annotations. For extension of the

network of PPI disclosed in the present study, PPI of human prey proteins, up to 10 for each prey of each bait set, were retrieved from the STRING database[12] and merged with the original PPI network deduced from Y2H and GR assay (present study only). Gene ontology terms were retrieved for the extended version of individual bait sets using g:Profiler[11]. **a,** A subset of the most statistically significant GO-Biological pathways, along with their associated p-value, is displayed for each extended bait set. **b,** Network representation and associated GO terms after extension. Each bait set of prey proteins is distinguished by functional "clouds" of a unique colour. Nodes representing human prey proteins disclosed by the Y2H and GR screen are filled, while nodes representing proteins added by String extension are unfilled.

Fig.5 **RNAi screen to identify TBEV host dependency and restriction factors. a,** Experimental workflow for the loss-of-function RNAi screen. **b,** A549 cells were transfected with an siRNA library and challenged with TBEV (MOI 0.5). Infectivity titers in the supernatant, 24h post-infection, were quantified by end-point dilution and normalized to infectivity titers obtained for cells transfected with nontargeted siRNA (Log_2 fold change). Data, expressed as $TCID_{50}$, are means of 2 biological replicates (with technical replicates). P-values were calculated by comparison of data obtained from cells transfected with targeted and nontargeted siRNA (Mann-Whitney test). Host dependency and host restriction factors revealed in the present study are marked in green and red, respectively, while positive controls for dependency and restriction factors (VIM and IFNAR2) are shown in yellow. **c,** TBEV-human host PPI network showing host dependency factors in green and host restriction factors in red.

SUPPLEMENTARY DATA

Supplementary Table 1: Summary of TBEV-*H. sapiens* protein-protein interactions (PPI) identified by yeast two-hybrid (Y2H) screening. Columns A and B display TBEV bait proteins and cognate human prey proteins, respectively, the latter referring to STRING identifiers. Uniprot identifiers and Uniprot protein descriptions are provided in columns C and D, respectively. Identification (+) or not (-) of the PPI in the Y2H screen is indicated in column E, and the number of yeast clones recovered for each PPI is indicated in column F. PPI that were evidenced by Gap repair (GR) assay, evaluated either because few yeast clones had been selected or because the PPI had been identified for LIV and the prey protein in question, are indicated in column G. Similarly, some PPI were evidenced by GR assay subsequent to their identification in a screen for PPI between TBEV and the bovine host, as indicated in column H. A summary of the evidence for each PPI (Y2H screen or GR assay or both) is provided in column I.

Supplementary Table 2: Bait sets and Extended bait sets. In order to return statistically significant Gene Ontology terms, bait sets for individual viral proteins were extended by the addition of up to ten PPI for each human prey of each bait set, as retrieved from the STRING database[12], using the Cytoscape StringApp[60].

Supplementary Table 3: Enriched Gene ontology terms for extended viral bait sets. Enriched gene ontology terms as regards Biological processes were retrieved for the STRING-extended version of individual using g:Profiler[11].

Supplementary Table 4: Sequence of siRNA used to knock down expression of genes encoding human proteins that physically interact with TBEV proteins, as determined in the Y2H screen described in the present study.

REFERENCES

1. Bogovic, P. & Strle, F. Tick-borne encephalitis: A review of epidemiology, clinical characteristics, and management. *World J Clin Cases* **3**, 430–441 (2015).
2. Rolland, T. *et al.* A proteome-scale map of the human interactome network. *Cell* **159**, 1212–1226 (2014).
3. Navratil, V., de Chassey, B., Combe, C. R. & Lotteau, V. When the human viral infectome and diseasome networks collide: towards a systems biology platform for the aetiology of human diseases. *BMC Syst Biol* **5**, 13 (2011).
4. Nicod, C., Banaei-Esfahani, A. & Collins, B. C. Elucidation of host-pathogen protein-protein interactions to uncover mechanisms of host cell rewiring. *Curr. Opin. Microbiol.* **39**, 7–15 (2017).
5. Carneiro, D. G., Clarke, T., Davies, C. C. & Bailey, D. Identifying novel protein interactions: Proteomic methods, optimisation approaches and data analysis pipelines. *Methods* **95**, 46–54 (2016).
6. Mairiang, D. *et al.* Identification of new protein interactions between dengue fever virus and its hosts, human and mosquito. *PLoS ONE* **8**, e53535 (2013).
7. Le Breton, M. *et al.* Flavivirus NS3 and NS5 proteins interaction network: a high-throughput yeast two-hybrid screen. *BMC Microbiol.* **11**, 234 (2011).
8. Shah, P. S. *et al.* Comparative Flavivirus-Host Protein Interaction Mapping Reveals Mechanisms of Dengue and Zika Virus Pathogenesis. *Cell* **175**, 1931-1945.e18 (2018).
9. Hafirassou, M. L. *et al.* A Global Interactome Map of the Dengue Virus NS1 Identifies Virus Restriction and Dependency Host Factors. *Cell Rep* **22**, 1364 (2018).
10. Kopecký, J., Křivanec, K. & Tomková, E. Attenuated temperature-sensitive mutants of tick-borne encephalitis virus isolated from natural focus. in *Modern Acarology* vol. 2 11–19 (SPB Academic Publ, 1991).
11. Raudvere, U. *et al.* g:Profiler: a web server for functional enrichment analysis and conversions of gene lists (2019 update). *Nucleic Acids Res* **47**, W191–W198 (2019).
12. Szklarczyk, D. *et al.* The STRING database in 2021: customizable protein-protein networks, and functional characterization of user-uploaded gene/measurement sets. *Nucleic Acids Res* **49**, D605–D612 (2021).
13. Liu, H. *et al.* Vimentin inhibits type I interferon production by disrupting the TBK1-IKKε-IRF3 axis. *Cell Rep* **41**, 111469 (2022).
14. Ambroggio, E. E., Costa Navarro, G. S., Pérez Socas, L. B., Bagatolli, L. A. & Gamarnik, A. V. Dengue and Zika virus capsid proteins bind to membranes and self-assemble into liquid droplets with

nucleic acids. *J Biol Chem* **297**, 101059 (2021).
15. Sotcheff, S. & Routh, A. Understanding Flavivirus Capsid Protein Functions: The Tip of the Iceberg. *Pathogens* **9**, E42 (2020).
16. Yamazaki, T. *et al.* Augmentation of drug-induced cell death by ER protein BRI3BP. *Biochem Biophys Res Commun* **362**, 971–975 (2007).
17. Ko, D. C. *et al.* Functional genetic screen of human diversity reveals that a methionine salvage enzyme regulates inflammatory cell death. *Proc Natl Acad Sci U S A* **109**, E2343-2352 (2012).
18. Mary, C. *et al.* Functional identification of APIP as human mtnB, a key enzyme in the methionine salvage pathway. *PLoS One* **7**, e52877 (2012).
19. Dodding, M. P. & Way, M. Coupling viruses to dynein and kinesin-1. *EMBO J* **30**, 3527–3539 (2011).
20. Lemasson, M. *et al.* Exploration of binary protein-protein interactions between tick-borne flaviviruses and Ixodes ricinus. *Parasit Vectors* **14**, 144 (2021).
21. Suzuki, T., Hirai, H. & Yoshida, M. Tax protein of HTLV-1 interacts with the Rel homology domain of NF-kappa B p65 and c-Rel proteins bound to the NF-kappa B binding site and activates transcription. *Oncogene* **9**, 3099–3105 (1994).
22. Gladue, D. P. *et al.* Interaction of CSFV E2 protein with swine host factors as detected by yeast two-hybrid system. *PLoS One* **9**, e85324 (2014).
23. Vuono, E. A. *et al.* SERTA Domain Containing Protein 1 (SERTAD1) Interacts with Classical Swine Fever Virus Structural Glycoprotein E2, Which Is Involved in Virus Virulence in Swine. *Viruses* **12**, E421 (2020).
24. Murata, T. *et al.* Epigenetic histone modification of Epstein-Barr virus BZLF1 promoter during latency and reactivation in Raji cells. *J Virol* **86**, 4752–4761 (2012).
25. Zaslavsky, E. *et al.* Antiviral response dictated by choreographed cascade of transcription factors. *J Immunol* **184**, 2908–2917 (2010).
26. Jantrapirom, S., Piccolo, L. L., Pruksakorn, D., Potikanond, S. & Nimlamool, W. Ubiquilin Networking in Cancers. *Cancers (Basel)* **12**, E1586 (2020).
27. Li, M. *et al.* Identification of antiviral roles for the exon-junction complex and nonsense-mediated decay in flaviviral infection. *Nat Microbiol* **4**, 985–995 (2019).
28. Gao, L. *et al.* Interaction with a ubiquitin-like protein enhances the ubiquitination and degradation of hepatitis C virus RNA-dependent RNA polymerase. *J Virol* **77**, 4149–4159 (2003).
29. Bouraï, M. *et al.* Mapping of Chikungunya virus interactions with host proteins identified nsP2 as a highly connected viral component. *J Virol* **86**, 3121–3134 (2012).
30. Lescar, J. *et al.* Towards the design of antiviral inhibitors against flaviviruses: the case for the multifunctional NS3 protein from Dengue virus as a target. *Antiviral Res* **80**, 94–101 (2008).
31. Luo, D., Lim, S. & Lescar, J. The Flavivirus NS3 Protein: Structure and Functions. *Molecular Virology and Control of Flaviviruses* 77–100 (2012).
32. Scholl, F. A., McLoughlin, P., Ehler, E., de Giovanni, C. & Schäfer, B. W. DRAL is a p53-responsive gene whose four and a half LIM domain protein product induces apoptosis. *J Cell Biol* **151**, 495–506 (2000).
33. Mille, F. *et al.* The Patched dependence receptor triggers apoptosis through a DRAL-caspase-9 complex. *Nat Cell Biol* **11**, 739–746 (2009).
34. Yang, T.-C. *et al.* Japanese encephalitis virus NS2B-NS3 protease induces caspase 3 activation and mitochondria-mediated apoptosis in human medulloblastoma cells. *Virus Res* **143**, 77–85 (2009).
35. Lin, J.-C. *et al.* Dengue viral protease interaction with NF-κB inhibitor α/β results in endothelial cell apoptosis and hemorrhage development. *J Immunol* **193**, 1258–1267 (2014).
36. Best, S. M. The Many Faces of the Flavivirus NS5 Protein in Antagonism of Type I Interferon Signaling. *J Virol* **91**, e01970-16 (2017).
37. Best, S. M. *et al.* Inhibition of interferon-stimulated JAK-STAT signaling by a tick-borne flavivirus and identification of NS5 as an interferon antagonist. *J Virol* **79**, 12828–12839 (2005).
38. Kellman, E. M., Offerdahl, D. K., Melik, W. & Bloom, M. E. Viral Determinants of Virulence in Tick-Borne Flaviviruses. *Viruses* **10**, E329 (2018).

39. Arif, A. *et al.* The GAIT translational control system. *Wiley Interdiscip Rev RNA* **9**, (2018).
40. Brass, A. L. *et al.* The IFITM proteins mediate cellular resistance to influenza A H1N1 virus, West Nile virus, and dengue virus. *Cell* **139**, 1243–1254 (2009).
41. Werme, K., Wigerius, M. & Johansson, M. Tick-borne encephalitis virus NS5 associates with membrane protein scribble and impairs interferon-stimulated JAK-STAT signalling. *Cell Microbiol* **10**, 696–712 (2008).
42. Guo, Y. *et al.* Structural basis for hijacking CBF-β and CUL5 E3 ligase complex by HIV-1 Vif. *Nature* **505**, 229–233 (2014).
43. Mack, G. J. & Compton, D. A. Analysis of mitotic microtubule-associated proteins using mass spectrometry identifies astrin, a spindle-associated protein. *Proc Natl Acad Sci U S A* **98**, 14434–14439 (2001).
44. Thein, K. H., Kleylein-Sohn, J., Nigg, E. A. & Gruneberg, U. Astrin is required for the maintenance of sister chromatid cohesion and centrosome integrity. *J Cell Biol* **178**, 345–354 (2007).
45. Khadka, S. *et al.* A physical interaction network of dengue virus and human proteins. *Mol Cell Proteomics* **10**, M111.012187 (2011).
46. Kesari, A. S. *et al.* Zika virus NS5 localizes at centrosomes during cell division. *Virology* **541**, 52–62 (2020).
47. Buchwalter, R. A. *et al.* Coordination of Zika Virus Infection and Viroplasm Organization by Microtubules and Microtubule-Organizing Centers. *Cells* **10**, 3335 (2021).
48. Coyaud, E. *et al.* Global Interactomics Uncovers Extensive Organellar Targeting by Zika Virus. *Mol Cell Proteomics* **17**, 2242–2255 (2018).
49. Gordon, D. E. *et al.* A SARS-CoV-2 protein interaction map reveals targets for drug repurposing. *Nature* **583**, 459–468 (2020).
50. Takano, A., Zochi, R., Hibi, M., Terashima, T. & Katsuyama, Y. Function of strawberry notch family genes in the zebrafish brain development. *Kobe J Med Sci* **56**, E220-230 (2011).
51. Takano, A., Zochi, R., Hibi, M., Terashima, T. & Katsuyama, Y. Expression of strawberry notch family genes during zebrafish embryogenesis. *Dev Dyn* **239**, 1789–1796 (2010).
52. Ferraris, P. *et al.* Zika virus differentially infects human neural progenitor cells according to their state of differentiation and dysregulates neurogenesis through the Notch pathway. *Emerg Microbes Infect* **8**, 1003–1016 (2019).
53. Pospisil, L., Jandasek, L. & Pesek, J. [Isolation of new strains of meningoencephalitis virus in the Brno region during the summer of 1953]. *Lek List* **9**, 3–5 (1954).
54. Sourisseau, M. *et al.* Deep Mutational Scanning Comprehensively Maps How Zika Envelope Protein Mutations Affect Viral Growth and Antibody Escape. *J Virol* **93**, e01291-19 (2019).
55. Reed, L. J. & Muench, H. A SIMPLE METHOD OF ESTIMATING FIFTY PER CENT ENDPOINTS. *Am J Epidemiol* **27**, 493–497 (1938).
56. Vidalain, P.-O. *et al.* A field-proven yeast two-hybrid protocol used to identify coronavirus-host protein-protein interactions. *Methods Mol Biol* **1282**, 213–229 (2015).
57. Fablet, A. *et al.* Comparative Virus-Host Protein Interactions of the Bluetongue Virus NS4 Virulence Factor. *Viruses* **14**, 182 (2022).
58. Walhout, A. J. & Vidal, M. High-throughput yeast two-hybrid assays for large-scale protein interaction mapping. *Methods* **24**, 297–306 (2001).
59. Shannon, P. *et al.* Cytoscape: a software environment for integrated models of biomolecular interaction networks. *Genome Res.* **13**, 2498–2504 (2003).
60. Doncheva, N. T., Morris, J. H., Gorodkin, J. & Jensen, L. J. Cytoscape StringApp: Network Analysis and Visualization of Proteomics Data. *J Proteome Res* **18**, 623–632 (2019).
61. Supek, F., Bošnjak, M., Škunca, N. & Šmuc, T. REVIGO summarizes and visualizes long lists of gene ontology terms. *PLoS One* **6**, e21800 (2011).

a

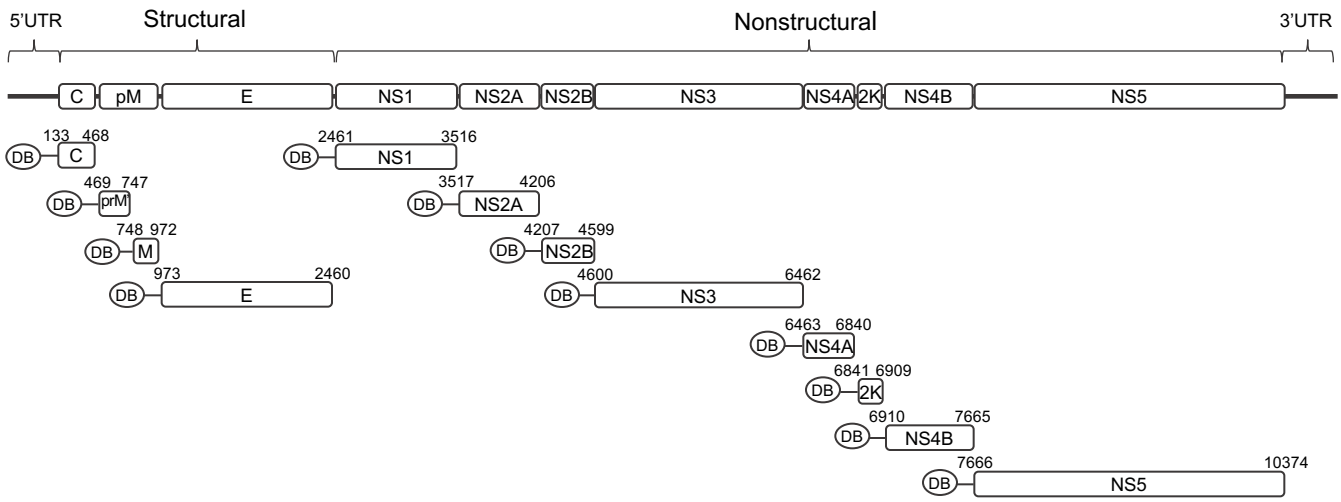
5'UTR
Structural
Nonstructural
3'UTR
C
pM
E
NS1
NS2A
NS2B
NS3
NS4A
2K
NS4B
NS5
DB
133 468
C
469 747
prM
748 972
M
973 2460
E
2461 3516
NS1
3517 4206
NS2A
4207 4599
NS2B
4600 6462
NS3
6463 6840
NS4A
6841 6909
2K
6910 7665
NS4B
7666 10374
NS5

b

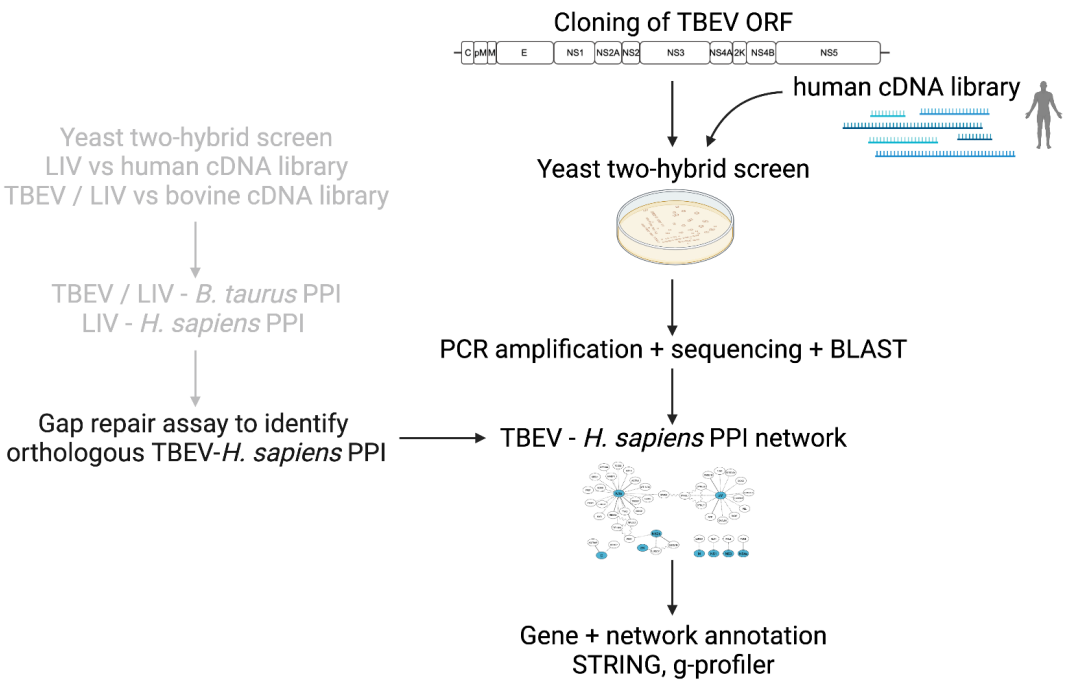
Cloning of TBEV ORF
human cDNA library
Yeast two-hybrid screen
Yeast two-hybrid screen
LIV vs human cDNA library
TBEV / LIV vs bovine cDNA library
TBEV / LIV - B. taurus PPI
LIV - H. sapiens PPI
PCR amplification + sequencing + BLAST
Gap repair assay to identify
orthologous TBEV-H. sapiens PPI
TBEV - H. sapiens PPI network
Gene + network annotation
STRING, g-profiler

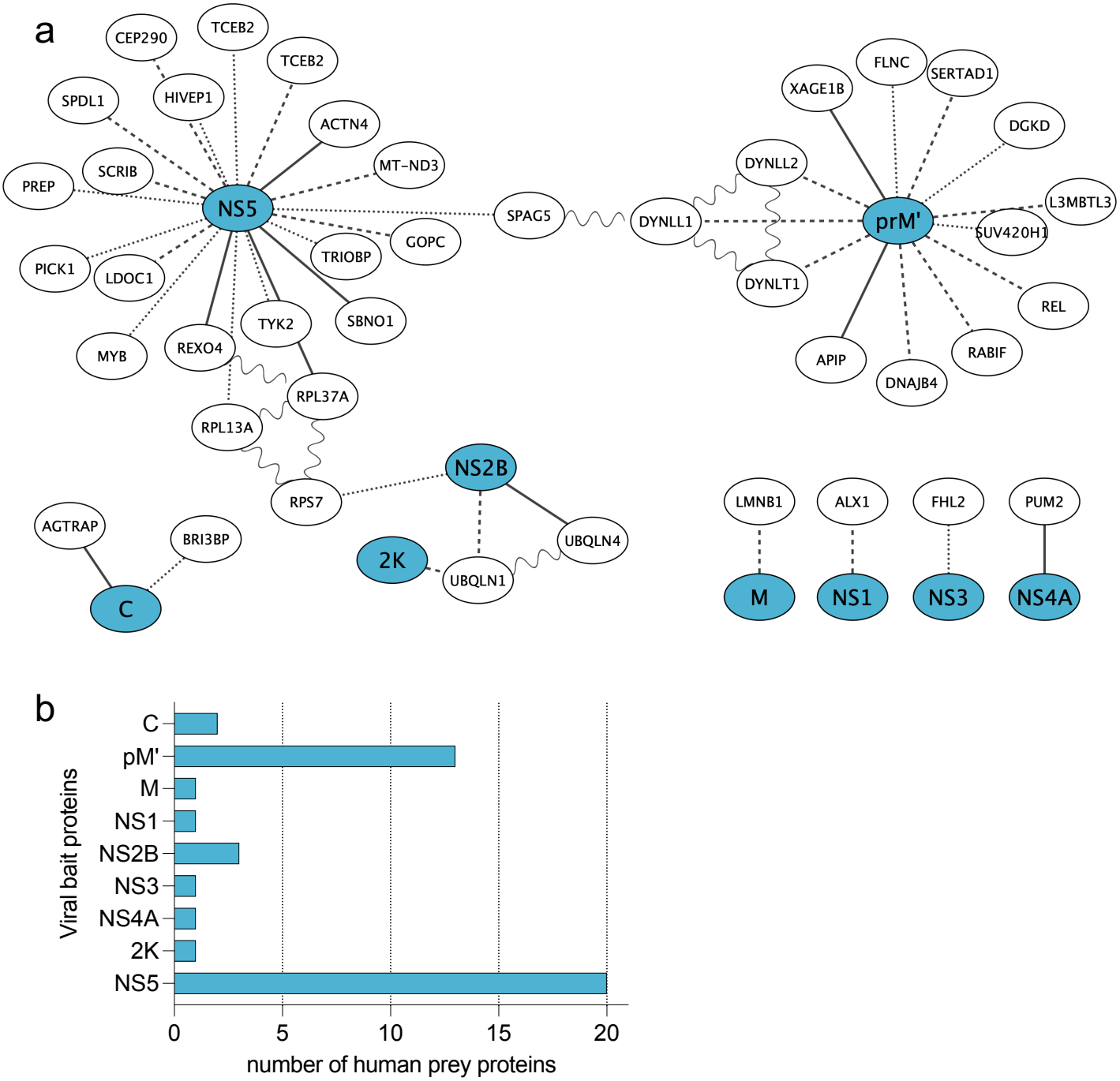
a
CEP290
TCEB2
TCEB2
SPDL1
HIVEP1
ACTN4
MT-ND3
PREP
SCRIB
NS5
SPAG5
GOPC
TRIOBP
PICK1
LDOC1
TYK2
SBNO1
MYB
REXO4
RPL37A
RPL13A
RPS7
NS2B
AGTRAP
BRI3BP
C
2K
UBQLN1
UBQLN4
FLNC
SERTAD1
XAGE1B
DGKD
DYNLL2
L3MBTL3
DYNLL1
prM'
SUV420H1
DYNLT1
REL
APIP
RABIF
DNAJB4
LMNB1
ALX1
FHL2
PUM2
M
NS1
NS3
NS4A
b
Viral bait proteins
C
pM'
M
NS1
NS2B
NS3
NS4A
2K
NS5
0
5
10
15
20
number of human prey proteins

Figure 2

a

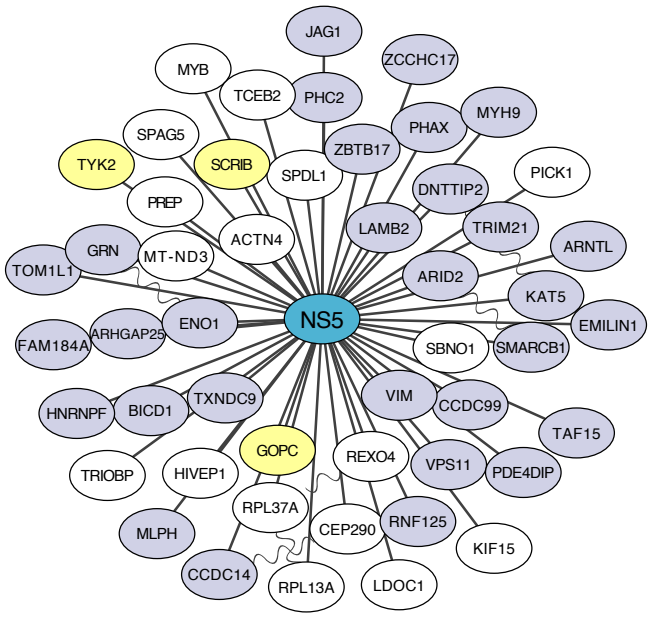
JAG1
ZCCHC17
MYB
TCEB2
PHC2
MYH9
PHAX
SPAG5
ZBTB17
TYK2
SCRIB
SPDL1
PICK1
DNTTIP2
PREP
LAMB2
TRIM21
ACTN4
ARNTL
GRN
MT-ND3
TOM1L1
ARID2
KAT5
NS5
EMILIN1
ENO1
ARHGAP25
FAM184A
SBNO1
SMARCB1
VIM
CCDC99
TXNDC9
HNRNPF
BICD1
TAF15
GOPC
REXO4
VPS11
PDE4DIP
TRIOBP
HIVEP1
RPL37A
RNF125
CEP290
MLPH
KIF15
CCDC14
RPL13A
LDOC1

b

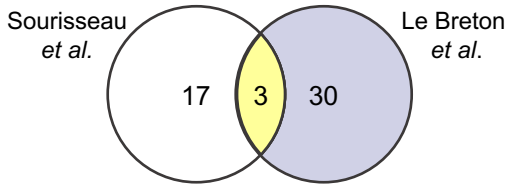
Sourisseau
et al.
Le Breton
et al.
17
3
30

Figure 3

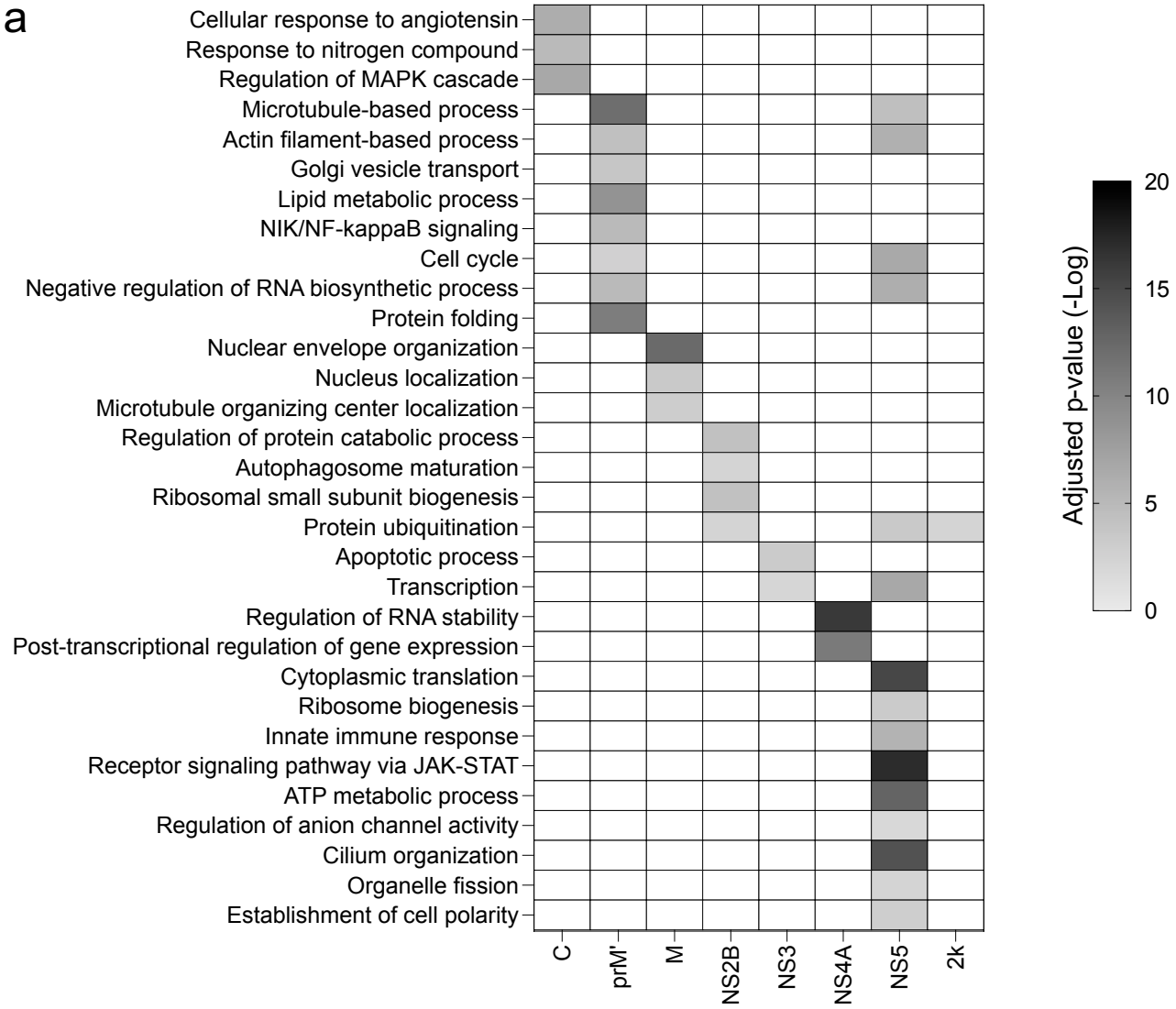
a
Cellular response to angiotensin
Response to nitrogen compound
Regulation of MAPK cascade
Microtubule-based process
Actin filament-based process
Golgi vesicle transport
Lipid metabolic process
NIK/NF-kappaB signaling
Cell cycle
Negative regulation of RNA biosynthetic process
Protein folding
Nuclear envelope organization
Nucleus localization
Microtubule organizing center localization
Regulation of protein catabolic process
Autophagosome maturation
Ribosomal small subunit biogenesis
Protein ubiquitination
Apoptotic process
Transcription
Regulation of RNA stability
Post-transcriptional regulation of gene expression
Cytoplasmic translation
Ribosome biogenesis
Innate immune response
Receptor signaling pathway via JAK-STAT
ATP metabolic process
Regulation of anion channel activity
Cilium organization
Organelle fission
Establishment of cell polarity
C
prM'
M
NS2B
NS3
NS4A
NS5
2k
Adjusted p-value (-Log)
20
15
10
5
0

Figure 4

Figure 4

b

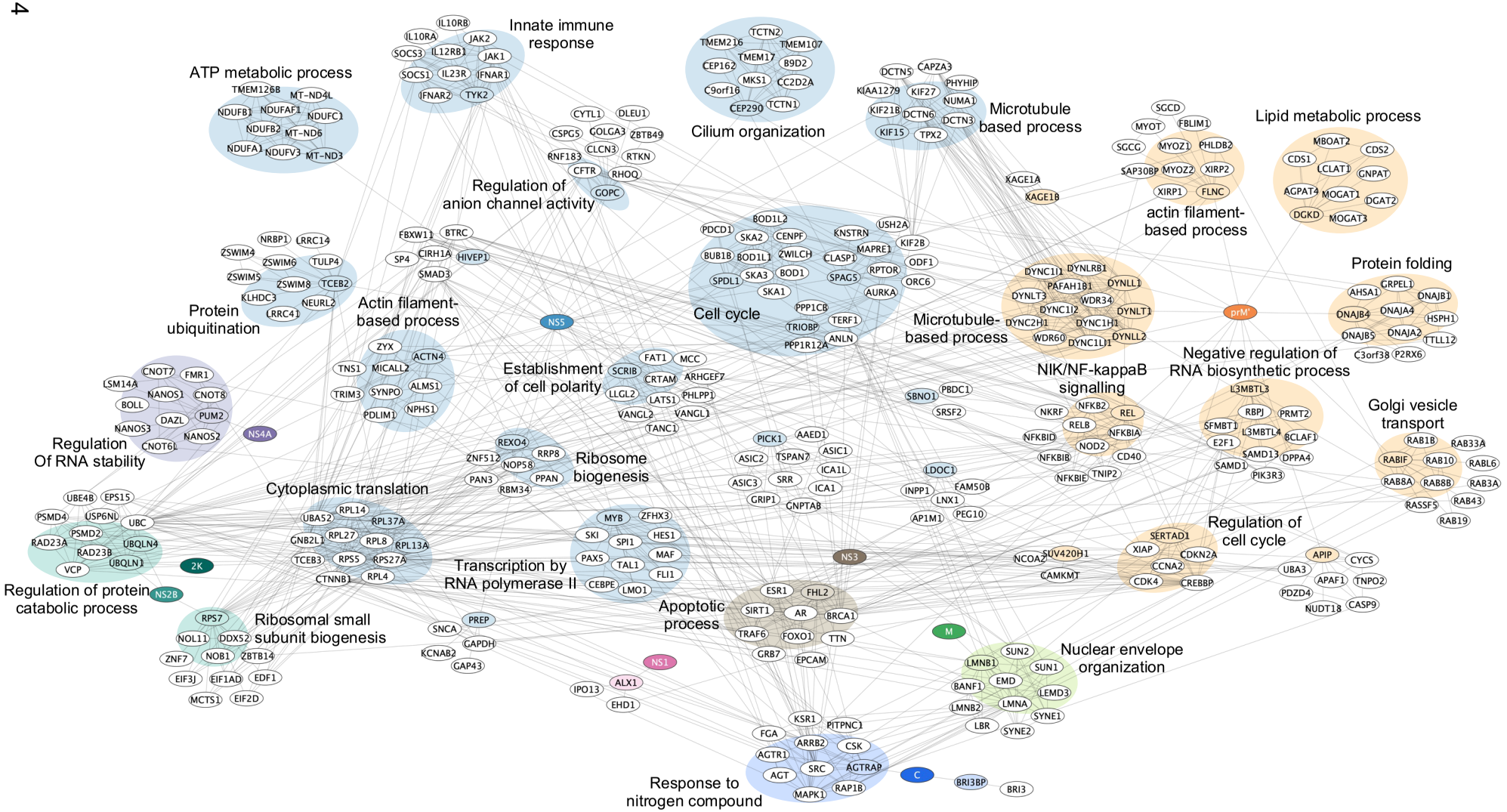
ATP metabolic process
TMEM126B
MT-ND4L
NDUFB1
NDUFAF1
NDUFC1
NDUFB2
MT-ND6
NDUFA1
NDUFV3
MT-ND3
Innate immune response
IL10RB
IL10RA
JAK2
SOCS3
IL12RB1
JAK1
SOCS1
IL23R
IFNAR1
IFNAR2
TYK2
Cilium organization
TMEM216
TCTN2
TMEM107
TMEM17
CEP162
B9D2
MKS1
CC2D2A
C9orf16
CEP290
TCTN1
Microtubule based process
DCTN5
CAPZA3
KIAA1279
KIF27
PHYHIP
NUMA1
KIF21B
DCTN6
DCTN3
KIF15
TPX2
Lipid metabolic process
SGCD
MYOT
FBLIM1
SGCG
MYOZ1
PHLDB2
SAP30BP
MYOZ2
XIRP2
XIRP1
FLNC
MBOAT2
CDS2
CDS1
LCLAT1
GNPAT
AGPAT4
MOGAT1
DGAT2
DGKD
MOGAT3
actin filament-based process
Regulation of anion channel activity
CYTL1
DLEU1
CSPG5
COLGA3
ZBTB49
CLCN3
RNF183
RTKN
CFTR
RHOQ
GOPC
KAGE1A
KAGE1B
Protein ubiquitination
NRBP1
LRRC14
ZSWIM4
ZSWIM6
TULP4
ZSWIM5
ZSWIM8
TCEB2
KLHDC3
NEURL2
LRRC41
Actin filament-based process
FBXW11
BTRC
SP4
CIRH1A
HIVEP1
SMAD3
NS5
Cell cycle
BOD1L2
PDCD1
SKA2
CENPF
KNSTRN
USH2A
KIF2B
BUB1B
BOD1L1
ZWILCH
CLASP1
MAPRE1
ODF1
SPDL1
SKA3
BOD1
SPAG5
RPTOR
ORC6
SKA1
AURKA
PPP1CB
TRIOBP
TERF1
PPP1R12A
ANLN
Microtubule-based process
DYNC1I1
DYNLRB1
PAFAH1B1
DYNLL1
DYNLT3
WDR34
DYNC1I2
DYNLT1
DYNC2H1
DYNC1H1
WDR60
DYNC1LI1
DYNLL2
prM'
Protein folding
AHSA1
GRPEL1
DNAJB1
DNAJB4
DNAJA4
HSPH1
DNAJB5
DNAJA2
TTLL12
C3orf38
P2RX6
Negative regulation of RNA biosynthetic process
Regulation Of RNA stability
CNOT7
FMR1
LSM14A
NANOS1
CNOT8
BOLL
DAZL
PUM2
NANOS3
NANOS2
CNOT6L
NS4A
ZYX
ACTN4
TNS1
MICALL2
TRIM3
SYNPO
ALMS1
PDLIM1
NPHS1
Establishment of cell polarity
FAT1
MCC
SCRIB
CRTAM
ARHGEF7
LLGL2
LATS1
PHLPP1
VANGL2
VANGL1
TANC1
NIK/NF-kappaB signalling
SBNO1
PBDC1
SRSF2
NKRF
NFKB2
REL
RELB
NFKBIA
NFKBID
NOD2
CD40
NFKBIB
TNIP2
NFKBIE
L3MBTL3
RBPJ
PRMT2
SFMBT1
L3MBTL4
BCLAF1
E2F1
SAMD13
DPPA4
SAMD1
PIK3R3
Golgi vesicle transport
RAB1B
RAB33A
RABIF
RAB10
RABL6
RAB8A
RAB8B
RAB3A
RASSF5
RAB43
RAB19
Ribosome biogenesis
REXO4
RRP8
ZNF512
NOP58
PAN3
PPAN
RBM34
PICK1
AAED1
ASIC2
TSPAN7
ASIC1
ICA1L
ASIC3
SRR
ICA1
GRIP1
GNPTAB
LDOC1
INPP1
FAM50B
LNX1
AP1M1
PEG10
Cytoplasmic translation
UBE4B
EPS15
PSMD4
USP6NL
UBC
PSMD2
RAD23A
UBQLN4
RAD23B
UBQLN1
VCP
2K
Regulation of protein catabolic process
NS2B
UBA52
RPL14
RPL37A
GNB2L1
RPL27
RPL8
RPL13A
TCEB3
RPS5
RPS27A
CTNNB1
RPL4
Transcription by RNA polymerase II
MYB
ZFHX3
SKI
SPI1
HES1
PAX5
TAL1
MAF
FLI1
CEBPE
LMO1
NS3
Regulation of cell cycle
NCOA2
SUV420H1
CAMKMT
SERTAD1
XIAP
CDKN2A
CCNA2
CDK4
CREBBP
APIP
CYCS
UBA3
APAF1
TNPO2
PDZD4
NUDT18
CASP9
Ribosomal small subunit biogenesis
RPS7
NOL11
DDX52
ZNF7
NOB1
ZBTB14
EIF3J
EIF1AD
EDF1
MCTS1
EIF2D
PREP
SNCA
GAPDH
KCNAB2
GAP43
Apoptotic process
ESR1
FHL2
SIRT1
AR
BRCA1
TRAF6
FOXO1
TTN
GRB7
EPCAM
M
Nuclear envelope organization
SUN2
LMNB1
SUN1
BANF1
EMD
LEMD3
LMNB2
LMNA
SYNE1
LBR
SYNE2
NS1
IPO13
ALX1
EHD1
Response to nitrogen compound
KSR1
PITPNC1
FGA
ARRB2
CSK
AGTR1
AGT
SRC
AGTRAP
MAPK1
RAP1B
C
BRI3BP
BRI3

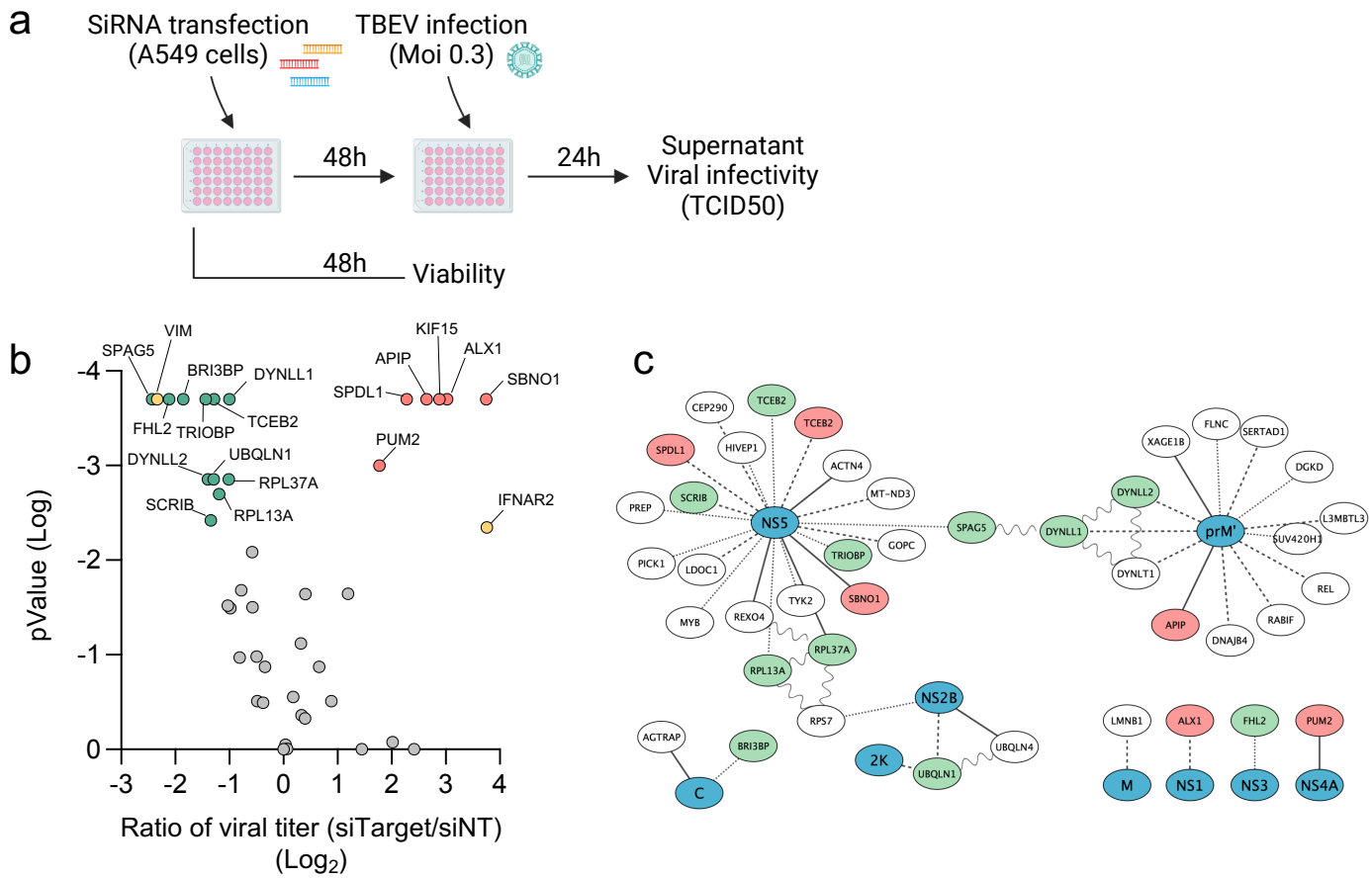
a
SiRNA transfection
(A549 cells)
TBEV infection
(Moi 0.3)
48h
24h
Supernatant
Viral infectivity
(TCID50)
48h
Viability
b
SPAG5
VIM
BRI3BP
DYNLL1
FHL2
TRIOBP
TCEB2
DYNLL2
UBQLN1
RPL37A
SCRIB
RPL13A
KIF15
APIP
ALX1
SPDL1
SBNO1
PUM2
IFNAR2
pValue (Log)
Ratio of viral titer (siTarget/siNT)
(Log2)
c
NS5
prM'
NS2B
2K
C
M
NS1
NS3
NS4A
CEP290
TCEB2
SPDL1
HIVEP1
ACTN4
MT-ND3
PREP
SCRIB
GOPC
TRIOBP
PICK1
LDOC1
TYK2
SBNO1
MYB
REXO4
RPL37A
RPL13A
RPS7
AGTRAP
BRI3BP
UBQLN4
UBQLN1
SPAG5
DYNLL1
DYNLL2
DYNLT1
FLNC
SERTAD1
XAGE1B
DGKD
L3MBTL3
SUV420H1
REL
RABIF
DNAJB4
APIP
LMNB1
ALX1
FHL2
PUM2

Figure 5